Int J Clin Exp Pathol 2016;9(8):8478-8484
www.ijcep.com /ISSN:1936-2625/IJCEP0031315

Original Article

Biological changes of myoepithelial cells in atrophic glands after ligation of parotid duct

Jinhua Zuo[1], Changling Ding[1], Yuhong Zhu[2], Lifang Wang[1], Duowen Liu[1]

Departments of [1]Oral and Maxillofacial Surgery, [2]Pathology, The Affiliated Hospital of Binzhou Medical College, Binzhou 256603, Shandong, China

Received April 27, 2016; Accepted June 22, 2016; Epub August 1, 2016; Published August 15, 2016

Abstract: Objective: We investigated the proliferative changes of myoepithelial cells (MECs) in atrophic glands after ligation of the parotid duct in rats. Methods: Seventy-eight Wistar rats were used as experimental animals and the main duct of the right parotid gland of each rat was ligated. Tissue samples of the parotid gland were taken from each group after 0 (control), 1, 3, 5, 7, 14, 21, and 30 days; histological changes in the parotid gland were examined by hematoxylin and eosin staining (n = 6), and the proliferation and distribution of MECs at different time points after ligation were analyzed by immunohistochemical double-staining. Results: After ligation of the parotid duct, the hematoxylin and eosin staining results showed that alveolar cells gradually disappeared, while a large number of duct-like structures appeared; fibrous tissue in the parotid gland proliferated and was infiltrated with inflammatory cells. Quantitative analysis of immunohistochemical staining results indicated that MECs proliferated rapidly, reaching a peak on the 5th day, after which the proliferation rate of MECs decreased and was maintained at a low level after 30 days. At 180 days, few proliferating MECs were observed. Conclusions: After ligation of the parotid duct, the parotid gland gradually atrophied and MECs proliferated during the early stage; subsequently, the proliferation capacity of MECs decreased and eventually stopped.

Keywords: MEC, parotid, atrophy, duct ligation, immunohistochemical double staining

Introduction

The damage to salivary gland tissue and the occurrence of salivary gland atrophy disease are induced by tumor radiotherapy of the head and neck [1], inflammation and trauma of the salivary gland [2], calculi obstruction of the gland duct, autoimmune disease (Sjogren's syndrome) [3], and degenerative lesions in the salivary gland. These conditions cause functional recession of the glands and decreases in saliva, seriously affecting the patient's oral health and quality of life. Current treatment methods for such diseases can only relieve symptoms by conventional drugs and cannot cure the conditions. Thus, how to effectively reverse atrophy and recover the function of the salivary gland is an urgent problem in clinical treatment. As one of the components of salivary glands, myoepithelial cells, (MECs) [4, 5] are mainly distributed in the acinar and between the glandular epithelium of small ducts and the basement membrane. MECs have a flat structure with characteristics of both smooth muscle and epithelial cells, which also determines the complexity of their biological functions. Previous studies showed that MECs could not only mechanically contract to promote secretion from human salivary glands [6], but also express multiple cytokines [7] involved in signal transduction, protecting the salivary gland by affecting the proliferation activity of MECs. Thus, numerous studies have suggested that MECs play an important role in promoting secretion from the salivary gland, resisting gland atrophy [8], and inhibiting tumors [9]. However, studies of MECs have mainly focused on their antitumor role, and few studies have examined the pathological process of gland atrophy. Therefore, in order to clarify the role of MEC in the process of gland atrophy, animal models of parotid gland atrophy after duct obstruction were established by inducing gradual atrophy of the gland through ligation of the parotid duct

[10, 11]. Morphological changes of the gland in the model group were observed and changes in MECs in the models with parotid gland atrophy were determined by immunohistochemical double staining; the proliferation rate of MECs at different time points was determined to explore the function of MECs in the process of parotid gland atrophy. Our results may provide a foundation for developing treatments for parotid gland atrophy.

Materials and methods

Animals and model

Seventy-eight healthy Wistar rats (male, weight 300±20 g) were purchased from the experimental animal center of Shandong University. They were randomly divided into 13 groups (6 rats in each group). Zero days was used as the negative control group. The effects of ligation of the parotid duct were examined in the experimental groups after 1, 3, 5, 7, 14, 21, 30, 60, 90, 120, 150, and 180 days. The rats were anaesthetized at different times of ligation, and then cut along the original surgical incision to locate the dominant duct of the parotid gland. The parotid along the dominant duct of the parotid and the right parotid gland were removed. Without ligating the parotid duct, the animals were sutured after removing the right parotid gland. The parotid gland was placed in 4% formaldehyde and paraffin specimens were prepared [12]. This study was carried out in strict accordance with the recommendations in the Guide for the Care and Use of Laboratory Animals of the National Institutes of Health. The animal use protocol has been reviewed and approved by the Institutional Animal Care and Use Committee (IACUC) of Binzhou Medical College.

Immunohistochemical double staining

Selection and collocation of double staining: In order to ensure the specificity of the reaction, the α-smooth muscle actin (SMA) and proliferating cell nuclear antigen (PCNA) antibodies (Abcam, Cambridge, UK) were used; the proteins detected and species origin of the two antigen were different. The experimental subjects were Wistar rats, and the primary antibodies included mouse monoclonal antibodies form mice and rabbits. Two different enzyme systems were applied in the study, including the BCIP/NBT alkaline phosphatase system and the AEC/peroxidase system, respectively. α-SMA monoclonal antibody (1:50) and PCNA monoclonal antibody (1:100) were used as the primary antibodies, and the DouMaxVision immunohistochemical double staining kit (Fuzhou Maixin Biotechnology Development, Fujian, China) was used as the secondary antibody. Parotid gland specimens were subjected to immunohistochemical double staining. The BCIP/NBT alkaline phosphatase and AEC/peroxidase systems were used for detection. Positive results for α-SMA and PCNA were blue-black and red, respectively; samples were re-stained by hematoxylin to observe the proliferation and morphological changes of MECs.

MEC count

Immunohistochemical sections were observed under a microscope (BXS1 Olympus type; Olympus, Tokyo, Japan). Five fields of view were randomly selected for each slice, and the number of double-positive MECs was counted suing Plus ImagePro 6 (Cybernetics Media, Rockville, MD, USA).

Statistical analysis

SPSS16.0 statistical software (SPSS, Inc., Chicago, IL, USA) was used to evaluate the data. The scores were expressed as $\bar{x} \pm s$; the means of different groups were compared by one-way analysis of variance, with $P < 0.05$ considered to indicate a statistically significant difference.

Results

Morphology

After ligation for 1 day, the volume of the ligated gland was significantly larger than that of the control group; edema occurred in the gland lobule and the boundary contour remained clear; edema of gland was relieved on the 3rd day, the volume of the gland decreased and atrophy was obvious on the 7th day, the gland was pale yellow, and there was no obvious difference from the normal parotid gland. The color of the parotid gland gradually deepened after 14-16 days and appeared to be dark gray; additionally, the glands became tough, the interval between the lobules became thick, and the edge of the skin was not clear. After 90 days of ligation, the gland was significantly reduced,

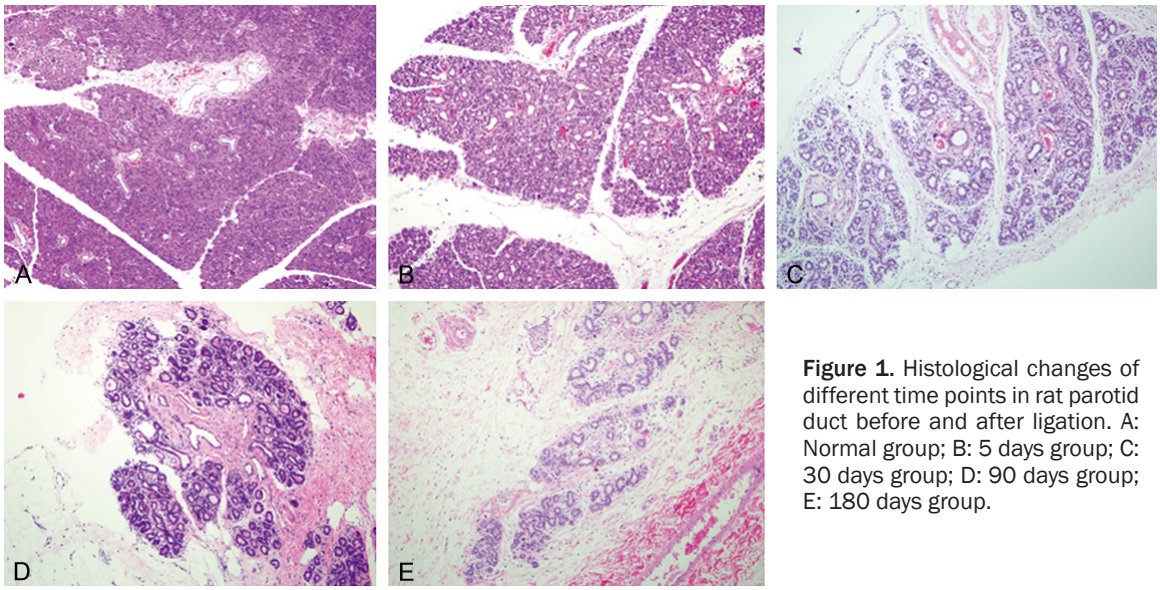

Figure 1. Histological changes of different time points in rat parotid duct before and after ligation. A: Normal group; B: 5 days group; C: 30 days group; D: 90 days group; E: 180 days group.

appeared to be gray, and the volume decreased to 1/3-1/2 of the size of the normal gland; for 150-180 days, the gland volume further reduced and the gland structure was completely invisible in the gland tissue.

Histology

The lobule of a normal parotid gland mainly consists of intensive serous alveolar cells and is widely scattered in the intercalated ducts and grain pipe, with a uniform acinar size and regular arrangement (**Figure 1A**). On the 1st day, the parenchyma of the parotid gland was similar to that of the normal parotid gland, except for duct expansion. On the 3rd day, the arrangement of the glandular leaflets gradually became disordered, but alveolar cells did not disappear. On the 5th day, catheter dilation was significantly increased (**Figure 1B**). On the 7th day, most of the cells were atrophic and the gap of the alveolar space was widened. The central part of the gland was severely atrophic and the edge region was visible; a catheter-like structure was obvious, lobules showed thickened intervals, and mononuclear cells had infiltrated. Moreover, hyperplasia of the fibrous tissue was observed and changes in the glandular tissue were obvious. Atrophy of the glands was severe at 14 days after ligation, the large catheter-like structure was increased, and infiltration of macrophages was observed in the surrounding residual duct-like structure. Fibrosis of lobule, an increase in collagen fibers, and infiltration of a large number of lymphocytes were observed accompanying the glass-like lesion. On the 21st day, the whole gland parenchyma contained a large number of duct-like structures and alveolar cells. After 30 days, the entire field of vision was filled with an expanded catheter-like structure, which was surrounded by fibrous connective tissue. The interval of the lobule was dense and contained a small number of drains filled with lymphocyte (**Figure 1C**). Sixty days later, the number of catheter-like structures was reduced and the structures showed irregular shapes. After 90-120 days, the shape of the large catheter-like structure was more obvious and the lumen was round (**Figure 1D**). At 150-180 days, the number of catheter-like structures and the number of abnormal vessels decreased. Extensive fibrosis of the gland parenchyma appeared and gradually replaced the glandular tissue; there was no obvious infiltration of lymphocytes (**Figure 1E**).

Immune phenotype

The proliferation and morphological changes of MECs were observed using the immunohistochemical double staining method. In the control group and the 1 day after ligation group, a small number of MECs (blue-black) could be seen around the acinus and intercalated duct (**Figure 2A**). Most MECs were in a non-proliferation stage. Based on the positive results for PCNA (red), that there were a small number of proliferating acinar cells and non-proliferating MECs

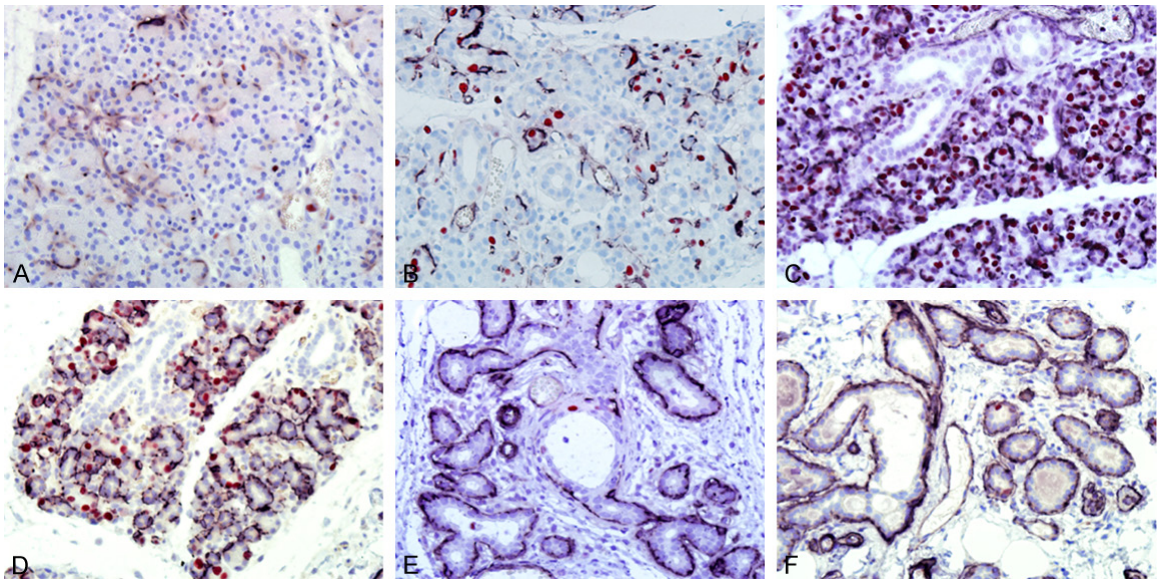

Figure 2. Double positive expression of PCNA and α-SMA in MEC of different time points in rat parotid duct before and after ligation. A: Normal group; B: 3 days group; C: 5 days group; D: 7 days group; E: 30 days group; F: 180 days group with DouMaxVision method.

Table 1. Proliferation rate of MEC at different time points in the process of parotid gland atrophy

Time of ligation (day)	Proliferation rate of MEC (%)
0	0.012±0.000
1	0.632±0.202*
3	2.492±0.262*
5	7.926±1.398*
7	4.868±1.016*
14	1.512±0.212*
21	0.714±0.093*
30	0.336±0.074*
60	0.318±0.163
90	0.106±0.033
120	0.168±0.124
150	0.064±0.087
180	0.000

Note: The significance of differences was determined by One-way ANOVA followed by Dunnett's test, presented as *$P < 0.05$ compared with control group.

were observed around the intercalated duct. On the 3rd day, MEC proliferation was obvious, with the proliferation of ductal epithelial cells; MECs attached to the surface of the acinar in a star shape and wrapped around the intercalated duct in a fusiform shape (**Figure 2B**). After 5 days, MEC proliferation was active based on microscope analysis and the number of MECs staining positive for PCNA significantly increased, accompanied by the proliferation of ductal epithelial cells (**Figure 2C**). At 7-14 days after ligation, MECs generally decreased, the number of acini decreased, and the catheter-like structure was increased (**Figure 2D**). After 21-30 days, the large catheter structure of the acinus gland was enclosed by MECs. The catheter-like structure showed a typical double-layer structure, with MECs mainly located in the outer layer (**Figure 2E**). After 60-90 days, the number of catheter-like structures reduced and had irregular shapes; the lumen of the catheter-like structure became round and regular, MECs were wrapped around the outer layer of the catheter-like structure, and double-positive MECs could not be easily observed after ligation for 150 days. After 180 days, no α-SMA and PCNA double-positive MECs were observed and the ductal epithelial cells were proliferating based on double-positive staining (**Figure 2F**).

Proliferation rate of MECs

The proliferation rates of MECs at different time points after ligation of the parotid duct are shown in **Table 1**. At 1-3 days after ligation, MECs began to proliferate rapidly, with the growth rate reaching a peak at 5 days and then decreasing; 30 days after ligation of the main duct, MECs were maintained at a low level. One-way analysis of variance was used to determine the proliferation rate of MECs at each

time point, which showed a normal distribution. The results of the Dunnett T3 test showed that the proliferation rate of the control group was significantly higher than that of the groups after ligation for 1, 3, 5, 7, 14, 21, and 30 days ($P < 0.05$). In the 1, 3, and 5 day groups, the proliferation rates of MECs were increasing, and the differences were statistically significant ($P < 0.05$); in groups of 7, 14, 21, and 30 days, the proliferation rates of MECs were decreasing, and the difference was statistically significant ($P < 0.05$). The proliferation rate of MECs was stable in groups of 30-180 days, and the difference was not statistically significant ($P > 0.05$).

Discussion

Atrophy of the salivary gland mainly occurs during the degeneration, atrophy, and disappearance of the acinus. This disease, which can develop after oral maxillofacial surgery, can seriously affect the oral health of patients, resulting in the disorders of patient's taste and eating. In this study, duct ligation was used to establish a rat model with salivary gland atrophy. Seven days after ligation, acinar cell atrophy was visible, the number of acinar cells was reduced, and catheter-like structures were increased in the rat model group. Compared with rats in the control group, the glandular structures of rats in the model group was reduced and the degree of damage to the glands increased over time after ligation, indicating that damage to the main duct in the salivary gland can injure the tissue of the salivary gland, which agrees with the results of Schilke *et al*. [13].

As important components of the salivary gland, MECs were previously shown to have an important role in the inhibition of parotid gland atrophy [14, 15]. Walker and Gobé [16] found that MECs gradually became obvious with gland atrophy and alveolar cell loss in rats with the atrophic parotid gland. Burgess *et al*. [5] confirmed that MECs inhibited gland atrophy to some degree based on immunohistochemical double staining. Similar results were observed in this study; the proliferation rates of MECs in the model group rats were 0.63%, 2.49%, and 7.92% at 1, 3, and 5 days after ligation, respectively. These results indicate that MEC proliferation is enhanced with increasing ligation time, suggesting that parotid gland injury participates in the induction of MEC proliferation. The proliferation rate of MECs in the model group decreased (4.86%) for 7 days after ligation and then decreased rapidly after ligation for 14-30 days. Combined with the morphological changes in the parotid gland observed in this study, we hypothesize that increased MEC activity is related to the early local inflammatory reaction [17], tissue edema, and increased pressure in the gland. In the late stage of duct obstruction (90 days), MECs still showed some proliferative activity, indicating that MECs can be used long-term to block the atrophy of the gland after the parotid gland atrophy. The results of previous studies examining MEC proliferation are controversial. Walker [18] suggested that the significant proliferation of MECs resulted from the induction of precursor cells. Batsakis *et al*. [19] found that MECs showed a very low proliferation rate, and even non-mitotic division may have occurred to a certain degree. However, Redman [20] observed that MECs differentiated during the mitotic division of parotid gland cells in mature rats based on transmission electron microscope analysis. In this study, we found that after injury, parotid gland tissue could promote MEC proliferation, suggesting that MECs have the potential to proliferate in parotid gland tissue. The reason for this may be related to the characteristics of the resistance to the catheter block and atrophy of the gland. With increasing glandular atrophy, MEC proliferation activity decreased and MECs were not observed in the parotid gland after 180 days, indicating that MECs had no proliferative activity. The number and occurrence of apoptosis of MECs decreased, but the mechanism requires further examination.

Immunohistochemical double staining is an advanced immunohistochemical staining technique that can be used to evaluate the expression of two different antigens in the same tissue section [21]. Few studies have applied this method to evaluate atrophic parotid disease in China. In this study, α-SMA and PCNA were selected as the markers for the antibodies, and good repeatability and stable results were observed. Changes in the proliferation of MECs in the atropic parotid gland were clearly observed, improving the objectivity and accuracy of judgment and adding clinical practical value.

In summary, in this study, rat models with parotid gland atrophy were successfully estab-

lished and the proliferation activity of MECs in the models with damaged parotid glands was evaluated. We found that MECs in the rat parotid gland showed low levels of proliferation and that proliferation was activated by salivary gland atrophy. The mechanism inducing MEC proliferation remains unclear, but the tendency towards proliferation decreased after activation in the atropic parotid gland. MECs can be used as therapeutic targets of glandular atrophy disease, and intervention is typically administered as corresponding drugs or other means, promoting the recovery of gland function; in contrast, in other cases (such as prevention of salivary fistula after parotidectomy), the antagonistic effect of gland function can be achieved by administering MEC-suppressing drugs to patients to promote residual gland and acinar atrophy and reduce patients' pain after long-term use of bandages. Therefore, the role of MECs in the process of parotid gland atrophy was clarified in this study.

Acknowledgements

This study was supported by Medical and Health Science and Technology Development Project of Shandong Province (2011HW004).

Disclosure of conflict of interest

None.

Address correspondence to: Jinhua Zuo, Department of Oral and Maxillofacial Surgery, The Affiliated Hospital of Binzhou Medical College, Binzhou 256603, Shandong, China. Tel: +86 13563058787; Fax: +86 543 3258850; E-mail: cnjhdoc@163.com

References

[1] Ou D, Zhang Y, He X, Gu Y, Hu C, Ying H, Zhu G, Wu Y, Mao J, Yue L and Shen X. Magnetic resonance sialography for investigating major salivary gland duct system after intensity-modulated radiotherapy of nasopharyngeal carcinoma. Int J Clin Oncol 2013; 18: 801-807.

[2] Dfacs ERC. 16. Trauma and Injuries to the Salivary Glands. Salivary Gland Pathology Diagnosis & Management; 2015. pp. 409-436.

[3] Turner MD. Salivary gland disease in Sjögren's syndrome: sialoadenitis to lymphoma. Oral Maxillofac Surg Clin North Am 2014; 26: 75-81.

[4] Jeong J, Baek H, Kim YJ, Choi Y, Lee H, Lee E, Kim ES, Hah JH, Kwon TK, Choi IJ and Kwon H. Human salivary gland stem cells ameliorate hyposalivation of radiation-damaged rat salivary glands. Exp Mol Med 2013; 45: e58.

[5] Palmer RM. The identification of myoepithelial cells in human salivary glands. A review and comparison of light microscopical methods. J Oral Pathol 1986; 15: 221-229.

[6] Ogawa Y. Immunocytochemistry of myoepithelial cells in the salivary glands. Prog Histochem Cytochem 2003; 38: 343-426.

[7] Ohtomo R, Mori T, Shibata S, Tsuta K, Maeshima AM, Akazawa C, Watabe Y, Honda K, Yamada T, Yoshimoto S, Asai M, Okano H, Kanai Y and Tsuda H. SOX10 is a novel marker of acinus and intercalated duct differentiation in salivary gland tumors: a clue to the histogenesis for tumor diagnosis. Mod Pathol 2013; 26: 1041-1050.

[8] Deugnier MA, Teulière J, Faraldo MM, Thiery JP and Glukhova MA. The importance of being a myoepithelial cell. Breast Cancer Res 2002; 4: 224-230.

[9] Sternlicht MD, Kedeshian P, Shao ZM, Safarians S and Barsky SH. The human myoepithelial cell is a natural tumor suppressor. Clin Cancer Res 1997; 3: 1949-1958.

[10] Fernandes LM, Teixeira FB, Alves-Junior SM, Pinheiro Jde J, Maia CS and Lima RR. Immunohistochemical changes and atrophy after chronic ethanol intoxication in rat salivary glands. Histol Histopathol 2015; 30: 1069-1078.

[11] Raz E, Saba L, Hagiwara M, Hygino de Cruz LC Jr, Som PM and Fatterpekar GM. Parotid gland atrophy in patients with chronic trigeminal nerve denervation. AJNR Am J Neuroradiol 2013; 34: 860-863.

[12] Takahashi S, Schoch E and Walker NI. Origin of acinar cell regeneration after atrophy of the rat parotid induced by duct obstruction. Int J Exp Pathol 1998; 79: 293-301.

[13] Schilke HK and Sapienza JS. Partial ligation of the transposed parotid duct at the level of the parotid gland for excessive salivary secretions. Vet Ophthalmol 2012; 15: 411-416.

[14] Tsujimura T, Ikeda R and Aiyama S. Changes in the number and distribution of myoepithelial cells in the rat parotid gland during postnatal development. Anat Embryol (Berl) 2006; 211: 567-574.

[15] Takahashi S, Nakamura S, Shinzato K, Domon T, Yamamoto T and Wakita M. Apoptosis and proliferation of myoepithelial cells in atrophic rat submandibular glands. J Histochem Cytochem 2001; 49: 1557-1564.

[16] Walker NI and Gobé GC. Cell death and cell proliferation during atrophy of the rat parotid gland induced by duct obstruction. J Pathol 1987; 153: 333-344.

[17] Hattori K, Murai N, Kusano J and Takahashi Y. Bilateral epithelial-myoepithelial carcinoma of the parotid glands. Head Neck 2016; 38: E73-75.
[18] Walker RA. Breast myoepithelium--the ignored cell. J Pathol 1988; 156: 5-6.
[19] Batsakis JG, Regezi JA, Luna MA and el-Naggar A. Histogenesis of salivary gland neoplasms: a postulate with prognostic implications. J Laryngol Otol 1989; 103: 939-944.
[20] Redman RS. Myoepithelium of salivary glands. Microsc Res Tech 1994; 27: 25-45.
[21] Fonseca-Alves CE, Bento DD, Torres-Neto R, Werner J, Kitchell B and Laufer-Amorim R. Ki67/KIT double immunohistochemical staining in cutaneous mast cell tumors from Boxer dogs. Res Vet Sci 2015; 102: 122-126.